PROBLEMY KOLEJNICTWA
RAILWAY REPORT Issue 193 (December 2021)
DOI: 10.36137/1934E
ISSN 0552-2145 (print) ISSN 2544-9451 (on-line)

Comparison of Fatigue Strength Calculation Methods for Monobloc Railway Wheels

Przemysław RAKOCZY[1], Robert BIŃKOWSKI[2]

Summary
EN 13979-1 "Railway applications – Wheelsets and bogies – Monobloc wheels – Technical approval procedure – Part 1: Forged and rolled wheels" approves two types of calculation models for determining fatigue strength – a 3D model and a simplified axially symmetric model with an asymmetric load. Both model types vary considerably, which may affect the results to be achieved. In addition, the determination of the maximum (critical) fatigue cycle amplitude for wheels requires stresses to be analysed at a point during the complete wheel revolution. In the current EN 13979-1 procedures, the amplitude is determined in the place and in the direction with the maximum principal stress without considering changes to stresses at a point for other wheel angular positions. The paper explains methods for strength calculations of monobloc wheels acc. to EN 13979-1. Both standard-approved models for the same wheel were developed and calculated. Differences, advantages and disadvantages of each model were described and the results compared. The complete load cycle for a given point on the wheel body was also analysed and presented. The results of the above analysis were analysed and further research directions were specified to define the actual maximum fatigue load cycle amplitude in railway wheels.

Keywords: monoblock railway wheels, fatigue strength, FEM analysis, fatigue load

1. Introduction

As opposed to tyred wheels, monobloc railway wheels are rolled or fully cast and machined partially (without wheel body) or fully. EN 13979-1 "Railway applications – Wheelsets and bogies – Monobloc wheels – Technical approval procedure – Part 1: Forged and rolled wheels" [1] defines requirements for monobloc wheels. In the first place, wheel fatigue strength is determined by analysing stresses using the finite element method (FEM). If the results of analytical calculations exceed the limit values, the wheel should be tested under a cyclic load [1].

The standard approves two models that can be prepared for FEM calculations – a complete 3D model and a simplified axially symmetric model with an asymmetric load (load in one section). Both model types vary considerably, which may affect the results to be achieved.

2. Procedure for strength calculations of monobloc wheels acc. to EN 13979-1

In all nodes of the wheel calculation model, two strength conditions must be met: static and fatigue. For the static condition, reduced stresses that cannot exceed the yield point are considered R_e.

The aim of fatigue analysis and the possible test specified by the standard is to determine the risk of a crack under a cyclic load for the entire useful life of the wheel. The first step is to analyse stresses to determine the maximum (critical) fatigue load cycle amplitude. If the analysis highlights the risk of a fatigue crack during the useful life of the wheel, the test should be performed. This paper only deals with the analytical part of the standard and, as the experience shows, meets requirements for the vast majority of analysed cases.

[1] Ph.D. Eng.; Railway Research Institute, Materials & Structure Laboratory; e-mail: prakoczy@ikolej.pl.
[2] M.Sc. Eng.; Railway Research Institute, Materials & Structure Laboratory; e-mail: rbinkowski@ikolej.pl.

2.1. External loads

To determine stresses, the standard defines a number of loads to be applied to the wheel model in the FEM. These stresses include not only external forces, but also assembly stresses caused by the pressure applied by the wheel to the axis. External loads are divided into 4 groups:

1. Straight track – no contract between the flanges and rail (vertical force);
2. Horizontal circular curve – contact between the inner part of the flange with the rail (horizontal and vertical force);
3. Turnout – contact between the inner part of the flange and the turnout check rail (horizontal and vertical force);
4. Extreme load.

Figure 1 shows locations where forces were applied in the model.

The standard also defines stresses caused by rotary wheel inertia. Due to the negligible impact compared to stresses caused by an external load and the pressure applied to the axis, stresses caused by rotary wheel inertia were omitted in the calculations described in this paper.

2.2. Strength calculations for a monobloc wheel

To determine the fatigue strength, principal stresses (σ_{max}) are determined for all points of the FEM grid and from all load cases. However, it should be mentioned that applying point forces of an external load causes unrealistically high stresses in the immediate vicinity of the force. In the real world, no force is applied to a point; instead, it is distributed across a certain area. This means that stresses for the running surface should be omitted. The running surface of the wheel is subject to other material fatigue processes related to frequent plastic deformations of the surface [2]. Once main stresses are determined, minimum stresses (σ_{min}) in direction σ_{max} from stress tensor (1), as shown in Figure 2, should be calculated. As tensor (1) is symmetric, it includes 6 components: three normal stresses (σ_{11}, σ_{22}, σ_{33}) and three shear stresses (σ_{12}, σ_{23}, σ_{31}).

$$\sigma_{ij} = \begin{bmatrix} \sigma_{11} & \sigma_{12} & \sigma_{13} \\ \sigma_{21} & \sigma_{22} & \sigma_{23} \\ \sigma_{31} & \sigma_{32} & \sigma_{33} \end{bmatrix} \tag{1}$$

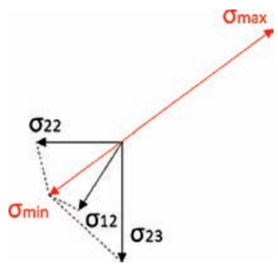

Fig. 2. Stress vector for determining σ_{min} [authors' own source]

To determine σ_{min}, the direction cosines of the stresses in the adopted Cartesian coordinate system must also be determined ($n\sigma_x$, $n\sigma_y$, $n\sigma_z$). σ_{min} can be calculated using Equation 2.

$$\sigma_{ij\min} = \begin{bmatrix} n\sigma_{ij\max}x & n\sigma_{ij\max}y & n\sigma_{ij\max}z \end{bmatrix} \times \\ \times \begin{bmatrix} \sigma_{11} & \sigma_{12} & \sigma_{13} \\ \sigma_{21} & \sigma_{22} & \sigma_{23} \\ \sigma_{31} & \sigma_{32} & \sigma_{33} \end{bmatrix} \times \begin{bmatrix} n\sigma_{ij\max}x \\ n\sigma_{ij\max}y \\ n\sigma_{ij\max}z \end{bmatrix}. \tag{2}$$

Once the maximum and minimum stresses are determined at each point and for each load case, the parameters of the fatigue load cycle, i.e. mean stresses (σ_m) and amplitude (σ_a) should be calculated using Equations 3 and 4 [1].

$$\sigma_m = \frac{\sigma_{\max} + \sigma_{\min}}{2}, \tag{3}$$

$$\sigma_a = \frac{\sigma_{\max} - \sigma_{\min}}{2}, \tag{4}$$

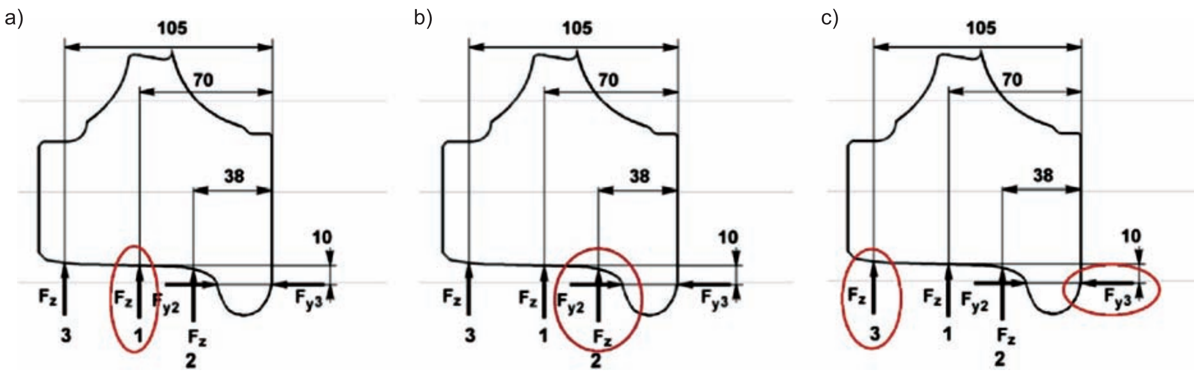

Fig. 1. Locations of force application: a) straight running, b) running on curves, c) turnout [authors' own source]

3. FEM analysis of a monobloc railway wheel

The FEM is currently the most common and applied method for engineering calculations. It is based on the discretisation of the geometry of a structure (division into a finite number of elements). With discretisation, complex geometry may be simplified to obtain relatively simple shapes for 3D analysis or planes for 2D analysis. Compared to the primary system, the discrete system has a finite number of degrees of freedom. Other system components are also discretised, i.e. the external load or boundary conditions. Then rigidity matroid *K*, inertia matrix *M* and attenuation matrix *C* are created, which, together with force vector *P*, form Equation (5) to be solved during FEM calculations [3–5].

$$M \times \ddot{x} + C \times \dot{x} + K \times x = P(t)\,. \qquad (5)$$

Therefore, in the FEM, the solution of complex differential equations of continuous functions is approximated with solving many algebraic equations.

For a railway wheel, the standard approves two models that can be prepared for FEM calculations – a complete 3D model and a simplified axially symmetric model with an asymmetric load (load in one section). If the structure of the wheel contains asymmetric elements (e.g. holes), no choice can be made – only a 3D model can be used. In the analysed case of a monobloc wheel, there are no asymmetric structural elements, so it was possible to develop a 3D model and an axially symmetric model. The model includes part of the axis together with the difference in the diameter of the axis and hub in order to calculate stresses caused by the pressure applied to the axis. As the axis is not the subject of the analysis, it was completed approx. 20 cm from the wheel and fixed in the entire cross-sectional plane.

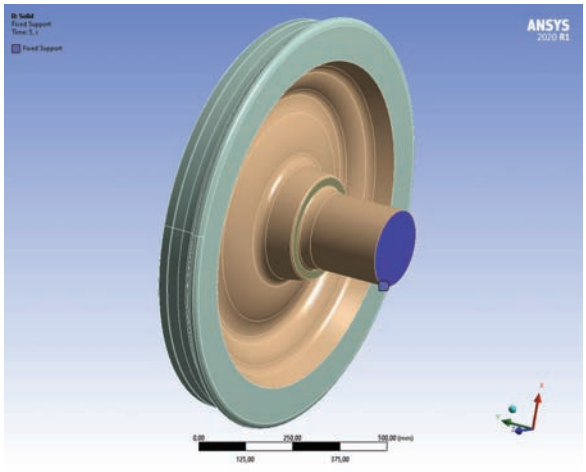

Fig. 3. 3D model of the wheel – fixed on the axis [authors' own source]

Fig. 4. 3D model of the wheel – grid [authors' own source]

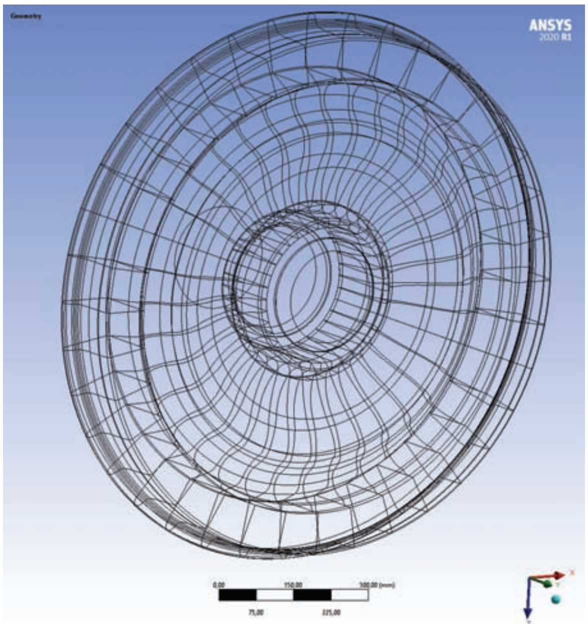

Fig. 5. Axially symmetric model of a monobloc wheel [authors' own source]

3.1. 3D model

The 3D model used cubic elements on the wheel body and hub as well as tetrahedral elements on the rim. The nominal size of all elements is 10 mm. Figure 3 and Figure 4 show the created 3D model of a monobloc wheel.

3.2. Axially symmetric model

The axially symmetric model includes 37 sections every 10 degrees in the rotation axis, which is a commonly used interval for analysing an axially symmetric model of a railway wheel. The nominal size of the elements is the same as for the 3D model – 10 mm.

4. Results of the analysis

The analysed models were subjected to the same cases of external forces, and stresses were calculated. For comparative analysis, radial and circumferential stresses for a cylindrical coordinate system, with the rotation axis in the wheel centre, were determined. Maximum principal stresses and von Mises stresses in the Cartesian coordinate system were also determined. For better result visibility, part of the hub and the entire rim near the wheel body were removed from the view. Examples of results for load case 2, i.e. curve, are shown in Figure 6 – Figure 9 for the 3D model and in Figure 10 – Figure 13 for the axially symmetric model.

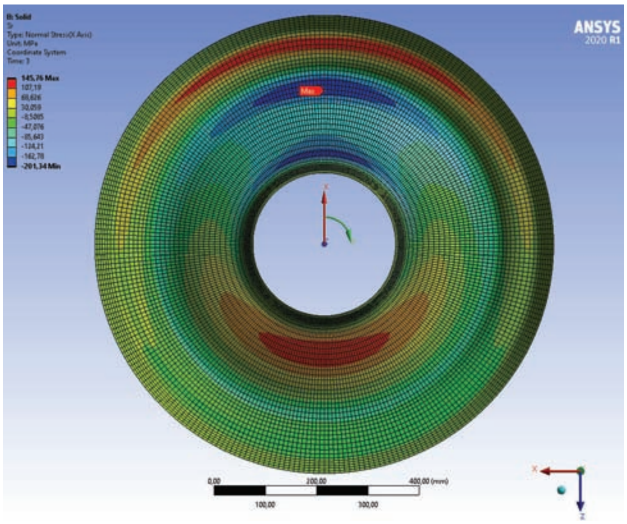

Fig. 6. 3D model – load case 2 – radial stresses [authors' own source]

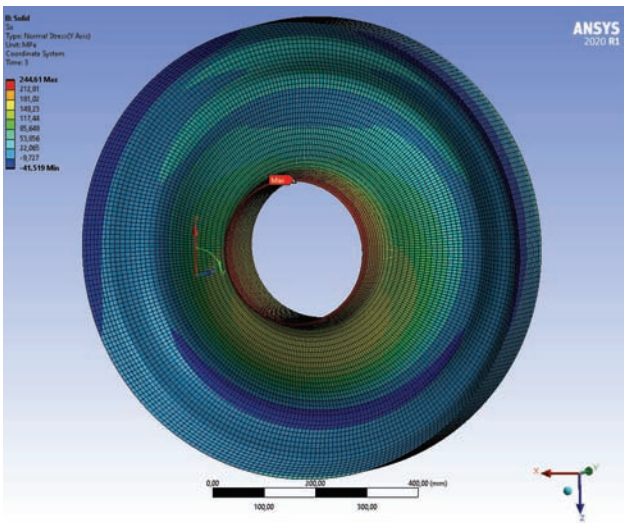

Fig. 7. 3D model – load case 2 – circumferential stresses [authors' own source]

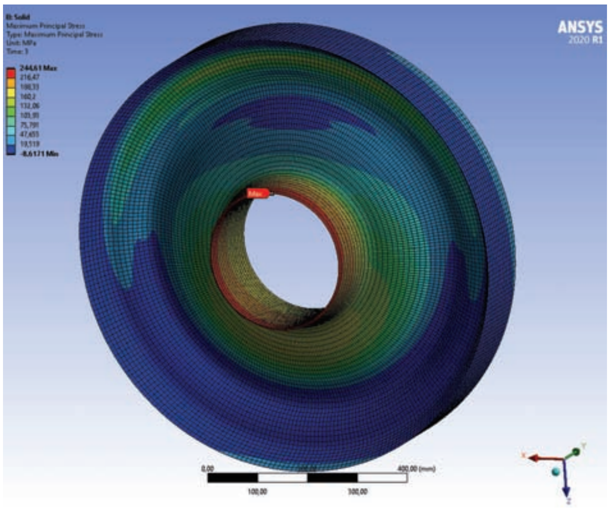

Fig. 8. 3D model – load case 2 – principal stresses [authors' own source]

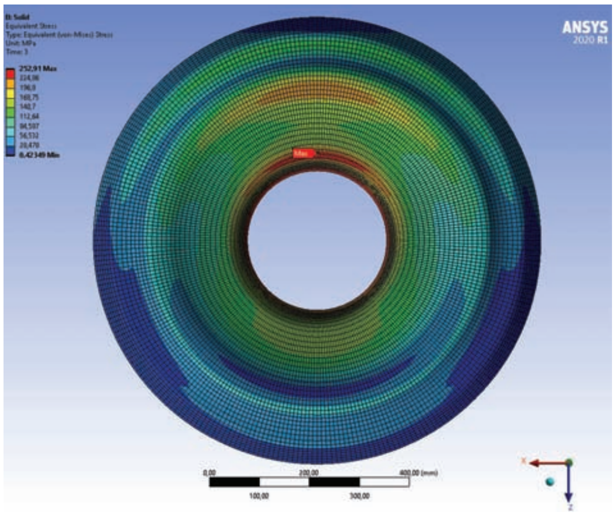

Fig. 9. 3D model – load case 2 – von Mises stresses [authors' own source]

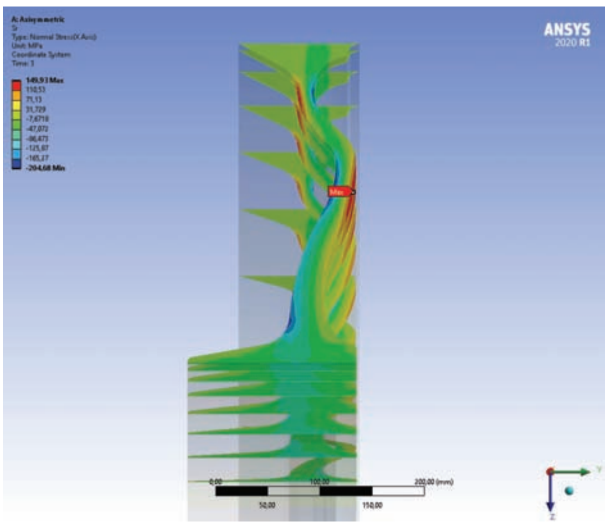

Fig. 10. Axially symmetric model – load case 2 – radial stresses [authors' own source]

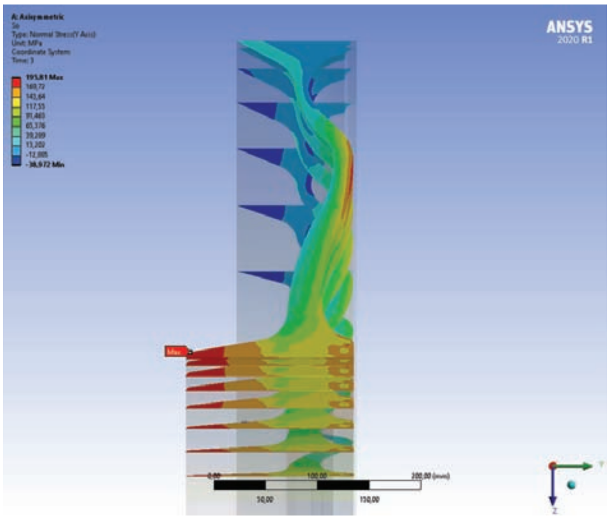

Fig. 11. Axially symmetric model – load case 2 – circumferential stresses [authors' own source]

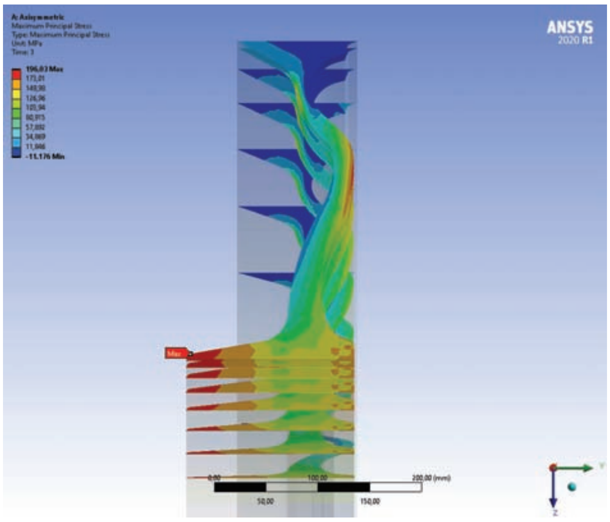

Fig. 12. Axially symmetric model – load case 2 – maximum principal stresses [authors' own source]

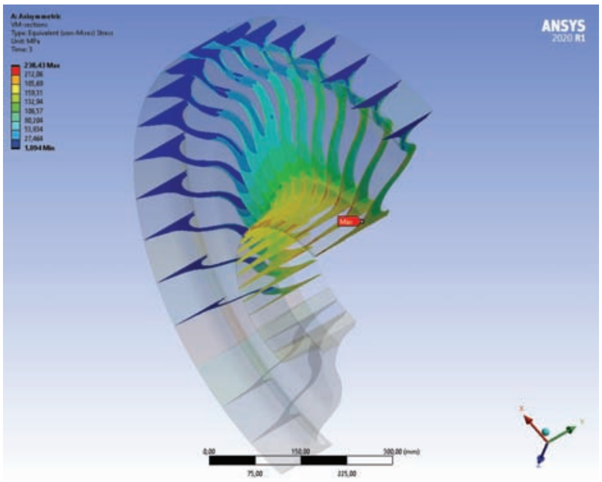

Fig. 13. Axially symmetric model – load case 2 – von Mises stresses [authors' own source]

The results for both analysed models are summarised in Table 1.

In extreme cases, the difference in the results is even 20%. For the largest differences, the 3D model points to higher stresses. The difference in the results when the axially symmetric model has higher stresses does not exceed 7%. The differences in the results may be caused by several factors:

- The main difference between the models is that the axially symmetric model provides results only for selected sections, which may not necessarily be locations with the highest stresses. By increasing the number of sections, the results of the axially symmetric model may be improved, but this will affect the calculation time.
- Another significant difference is the type of finite elements and, thus, their calculation method. For large models, this may have an impact on results.

Table 1

Stress comparison results

Load case	Stresses	3D model [MPa]	Axially symmetric model [MPa]	Difference [%]
1	Radial	96.5	103.1	6.8
2		145.8	149.9	2.8
3		149.6	153.28	2.5
1	Circumferential	237.5	194.2	18.2
2		244.6	195.8	20.0
3		237.1	193.7	18.3
1	Maximum principal	237.5	194.6	18.1
2		244.6	196	19.9
3		237.1	194.1	18.1
1	von Mises	238.8	201.7	15.5
2		252.9	238.4	5.7
3		265.1	274.47	3.5

[Authors' own source].

- Short calculation time is the unquestionable advantage of axially symmetric models. Therefore, making the grid denser does not extend the time needed to obtain results considerably. Making the element grid denser usually provides more accurate results, especially in areas where stresses are less concentrated. In this analysis, the axially symmetric model has the nominal element size to exclude this variable.

5. Load cycle analysis

The procedure for calculating the fatigue strength given in EN 13979-1 does not analyse the complete cyclic load applied to each wheel point. For practical reasons, the external load in the FEM analysis is fixed, while the test concerns each wheel point separately. Even though this type of analysis yields a full spectrum of stresses during the entire rotary motion cycle of the wheel as a whole, the determination of fatigue strength parameters for each point separately fails to consider this cycle. To determine the actual load cycle, coaxial points at each wheel cross-section height would have to be grouped. Figure 14 shows an example of a set of coaxial points. Each group of points forms a history of stresses during the complete wheel revolution. Figure 15 shows the stress history for an example of a group of points taken from Figure 14. In other words, during the complete wheel revolution, each point is subjected to stresses of any other point in its set. With this in mind, whole sets of points with the results of the FEM analysis would have to be analysed to determine the complete stress cycle. However, EN 13979-1 does not currently require such analysis to be conducted.

6. Conclusions

The comparative analysis of both types of FEM models approved by the current edition of the EN 13979-1 standard points to significant differences in results. Results for both models should meet when the grid in the 3D model becomes denser and the number of sections in the axially symmetric model increases. Also, the preliminary analysis of the history of stresses of coaxial points reveals that the methods for determining mean stresses (σ_m) and amplitude (σ_a) described in EN 13979-1 fails to consider the rotary motion cycle of the wheel entirely. This may lead to errors in the determination of fatigue cycle stresses and, as a result, to the overestimation of the fatigue strength of a wheel. The authors point to the need to conduct further analyses to estimate differences in the fatigue cycle determined acc. to the current EN 13979-1 requirements compared to the proposed method and considering sets of coaxial points.

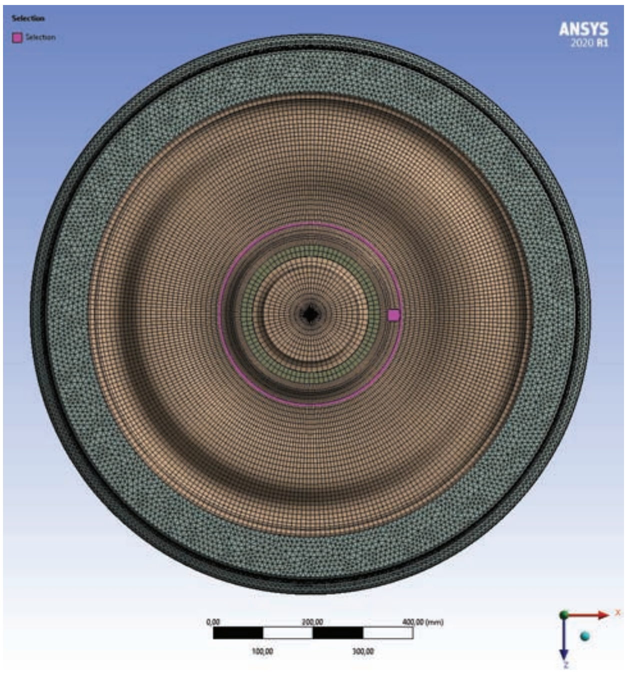

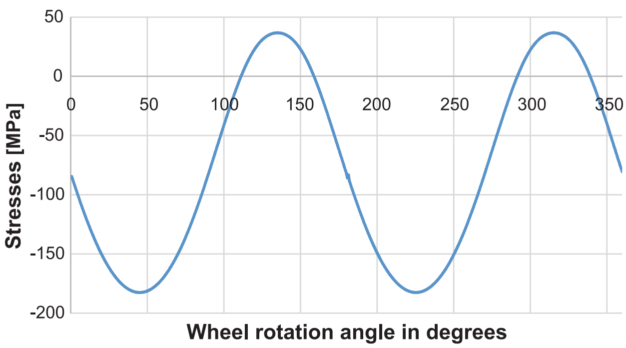

Fig. 15. Stress history for an example of a coaxial group of points [authors' own source]

Fig. 14. Example of a coaxial group of points on the wheel [authors' own source]

References

1. EN 13979-1:2011 "Railway applications – Wheelsets and bogies – Monoblock wheels – Technical approval procedure – Part 1: Forged and rolled wheels".
2. Mikłaszewicz I.: *Charakterystyczne uszkodzenia zestawu kołowego powodujące zdarzenia wypadkowe* [Characteristic damages of a wheelset causing accidents], Railway Reports, Warszawa, 2008.
3. Dacko M. et.al.: *Metoda Elementów Skończonych w mechanice konstrukcji* [Finite Element Method in structural mechanics], Arkady, Warszawa, 1994.
4. Rakowski G., Kacprzyk Z.: *MES w mechanice konstrukcji* [FEM in structural mechanics], Oficyna Wydawnicza Politechniki Warszawskiej, Warszawa, 2005.
5. Rusiński E., Czmochowski J., Smolnicki T.: *Zaawansowana metoda elementów skończonych w konstrukcjach nośnych* [Advanced finite element method in load-bearing structures], Oficyna Wydawnicza Politechniki Wrocławskiej, Wrocław, 2000.